Nuclear effects on lepton polarization in charged-current quasielastic neutrino scattering

M. Valverde,[1] J.E. Amaro,[1] J. Nieves,[1] and C. Maieron[2]

[1]*Departamento de Fisica Atomica, Molecular y Nuclear,*
Universidad de Granada, Granada 18071, Spain
[2]*INFN, Sezione di Catania, Via Santa Sofia 64, 95123 Catania, Italy*

We use a correlated local Fermi gas (LFG) model, which accounts also for long distance corrections of the RPA type and final-state interactions, to compute the polarization of the final lepton in charged-current quasielastic neutrino scattering. The present model has been successfully used in recent studies of inclusive neutrino nucleus processes and muon capture. We investigate the relevance of nuclear effects in the particular case of τ polarization in tau-neutrino induced reactions for several kinematics of relevance for neutrino oscillation experiments.

I. INTRODUCTION

The purpose of this paper is to investigate the importance of nuclear effects on the final lepton polarization in neutrino-induced charged-current (CC) inclusive reactions of the type (ν_l, l). In particular we present results for the tau polarization in (ν_τ, τ) reactions. The interest of these studies on neutrino-nucleus reactions lies on their implications for the neutrino oscillations experiments [1, 2] (see [3] and references therein for a recent review). Some of the experiments proposed to demonstrate the $\nu_\mu \to \nu_\tau$ oscillation are expecting to detect the τ production signal through the (ν_τ, τ^-) or $(\overline{\nu}_\tau, \tau^+)$ reactions [4, 5], among them the CNGS project [6], which will send a neutrino beam from CERN to the Gran Sasso laboratory, where the ICARUS and OPERA detectors will start taking data in the next few months. The τ decay particle distributions depend on the τ spin direction. Thus the theoretical information on the τ polarization will be valuable, since the expected number of ν_τ events will not be large [7, 8, 9]. The study of τ polarization is also needed, for instance, in $\nu_\mu \to \nu_e$ oscillation experiments to disentangle (ν_e, e) events from background electron production following the $\nu_\mu \to \nu_\tau$ oscillation [10].

The study of lepton polarization in (ν_l, l) and reactions is also of theoretical interest since the polarization observables may display peculiar sensitivities to the ingredients of the nuclear and reaction models, different to the ones shown by the cross sections. However the optimal neutrino-energy regime to obtain partially polarized leptons in non-longitudinal directions is limited. The reason is that for high energy (compared to it mass) the final leptons are 100% polarized with negative helicity. This is the case for the electrons in (ν_e, e) reactions for most of the energies involved in experiments. In the case of muon production for some moderate energies, a non negligible transverse polarization component, though small, could be observed, and some examples will be shown below in this paper. More interesting is the aforementioned case of tau leptons due to the large value of its mass. This lepton will be the main focus of this paper.

Previous studies of lepton polarization observables in neutrino induced reactions focus mainly on τ polarization from nucleon targets for a range of kinematics of interest [10]–[15].

Neutrino detectors are based on neutrino-nucleus interactions (such as Argon in the ICARUS experiment), and *a priori* one would need to evaluate the lepton polarization observables in actual finite nuclei models. Genuine nuclear physics effects are usually neglected in these kind of reactions, since relatively high energies are involved. However for low to intermediate energy transfer nuclear effects do play a role in the inclusive cross section of (ν, l) reactions and in general cannot be neglected (Pauli blocking, finite size effects, long and short-range correlations, final-state interactions, sub-nuclear degrees of freedom, etc.). This is well known from electron scattering studies, that usually are the starting point of neutrino scattering models. For the same kinematics the (e, e') reaction, and the (ν, l) reaction in the weak-vector sector are complementary to each other and make use of the same dynamical ingredients. Only the weak-axial current contribution makes a difference in the description of both reactions, since it can excite different nuclear modes.

Only if a given model is able to reproduce to some extent the available (e, e') data, its predictions for neutrino reactions can be considered reliable. Different theoretical approaches along these lines on neutrino reactions in nuclei can be found among the recent literature available [16, 17, 18, 19, 20, 21, 22, 23, 24, 25].

In this paper we describe the (ν_l, l) reaction within the many-body framework of refs. [26, 27]. Our model is an extension of previous studies on electron [28], photon [29], and pion [30, 31] interactions in nuclei. It is based on a Local Fermi Gas (LFG) description of the nucleus, accounting for Pauli blocking. The experimental Q-values are used to enforce a correct energy balance of the reaction. Additional nuclear effects, essential to describe e, γ and π reactions, are built on top of the model, in particular:

1. Coulomb distortion of the charged leptons,

2. Medium polarization, which is taken into account through the random-phase approximation (RPA),

3. Final-state interaction (FSI).

The model was first applied to neutrino reactions in Ref. [26], providing one of the best existing simultaneous description of inclusive muon capture, (ν_μ, μ^-) and (ν_e, e^-) reactions in ^{12}C near threshold. Inclusive muon capture from other nuclei was also successfully described by the model. Apart from the description of the absorption of real photons by nuclei [29], the model describes rather well the (e, e') inclusive cross section of ^{12}C, ^{40}Ca and ^{208}Pb for different kinematics, not only in the QE region, but also when extended to the $\Delta-$peak and the dip region [28]. Recently the model has been extended to the neutral current sector, and one-nucleon knock-out reactions have been studied both for CC and neutral current driven processes [32]. A special effort has also been paid in Ref. [27] to reliably estimate the theoretical uncertainty of our model.

In this paper we extend the above model to the calculation of lepton polarization components in CC neutrino reactions. To our knowledge, only one previous study exists analyzing nuclear effects on lepton polarization [33]. This model basically consists on a relativistic local Fermi gas (LFG) including nuclear dynamical corrections such as some kind of relativistic RPA correlations and an effective mass for the nucleons inside the nucleus (this is an approximate way of taking into account the FSI). However the model of [33], first presented in [34, 35], has not been tested in other nuclear reactions such as (e, e').

In Sect. 2 we introduce the formalism and discuss the kinematics of the (ν_l, l) reaction for muon and tau leptons in order to identify the most interesting cases. In Sect. 3 we

present results for differential cross sections and lepton polarization components, and draw our conclusions.

II. FORMALISM AND KINEMATICS

In this work we will study the inclusive neutrino-induced reaction depicted in Fig. 1. A neutrino ν_l (or anti-neutrino $\overline{\nu}_l$) with four momentum $K^\mu = (E_\nu, \vec{k})$ exchanges a W boson with an atomic nucleus with initial momentum $P^\mu = (M_i, \vec{0})$, and a polarized lepton l^- (or l^+) is detected with four-momentum $K'^\mu = (E'_l, \vec{k'})$. In the inclusive reaction the final hadronic state is not detected. In this work we deal with the quasielastic channel, where the main contribution is due to one-nucleon emission.
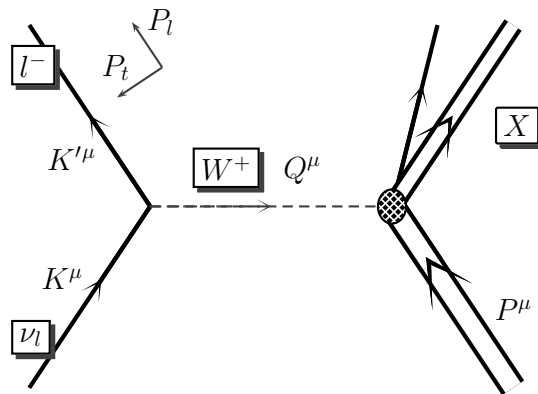

FIG. 1: Kinematics of the reaction, where we show the scattering plane and the directions of the two lepton polarization components P_l and P_t.

We write the unpolarized differential cross section as [26]

$$\Sigma_0 \equiv \frac{d^2\sigma_{\nu l}}{d\Omega' dE'_l} = \frac{|\vec{k'}|G^2 M_i}{2\pi^2}F, \tag{1}$$

where G is the Fermi weak coupling constant, Ω' is the solid angle of the final lepton, and the quantity F has been defined as

$$\begin{aligned}
F &= \left(2W_1 + \frac{m_l^2}{M_i^2}W_4\right)(E'_l - |\vec{k'}|\cos\theta) + W_2(E'_l + |\vec{k'}|\cos\theta) \\
&\quad - W_5\frac{m_l^2}{M_i} \mp \frac{W_3}{M_i}\left(E_\nu E'_l + |\vec{k'}|^2 - (E_\nu + E'_l)|\vec{k'}|\cos\theta\right)
\end{aligned} \tag{2}$$

resulting from the usual contraction between the leptonic and hadronic tensors. Here θ is the angle between $\vec{k}$ and $\vec{k'}$, and the $\mp$ sign in the last term correspond to the case of neutrino or anti-neutrino scattering. Finally the structure functions W_i are defined in the hadronic tensor as

$$\frac{W^{\mu\nu}}{2M_i} = -g^{\mu\nu}W_1 + \frac{P^\mu P^\nu}{M_i^2}W_2 + i\frac{\epsilon^{\mu\nu\gamma\delta}P_\gamma q_\delta}{2M_i^2}W_3 + \frac{q^\mu q^\nu}{M_i^2}W_4 + \frac{P^\mu q^\nu + P^\nu q^\mu}{2M_i^2}W_5 \tag{3}$$

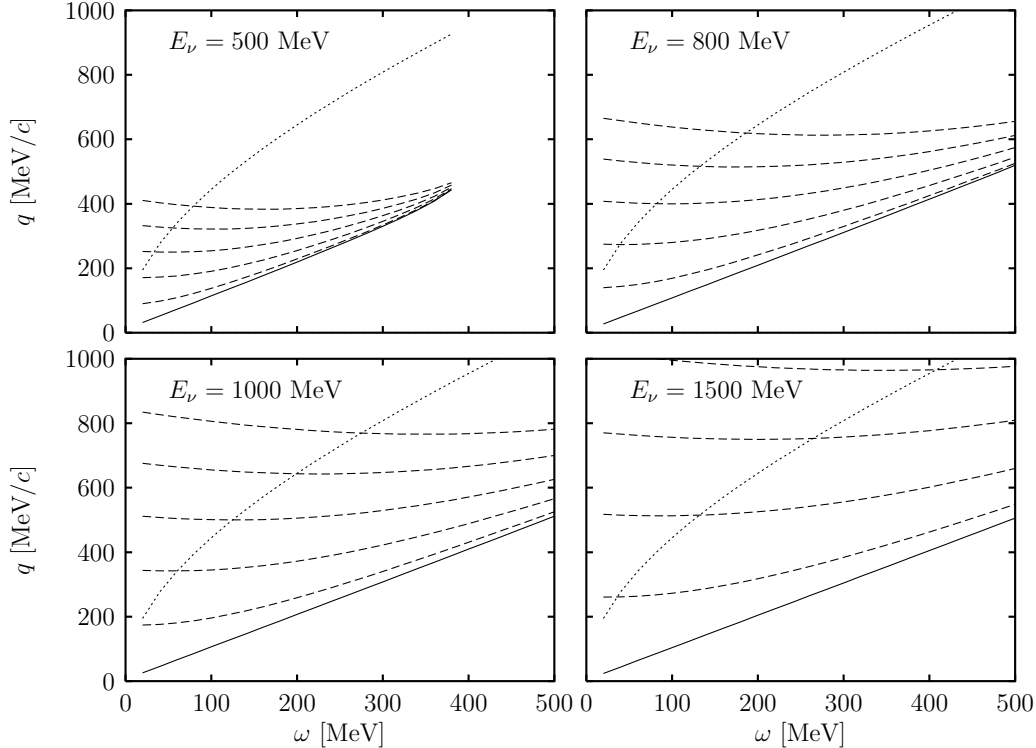FIG. 2: Allowed kinematics for (ν_μ, μ) reaction in the (ω, q) plane. The dotted line is the center of the quasielastic peak $\omega = (q^2 - \omega^2)/2m_N$. The other lines show in each panel the value of q as a function of ω for a fixed value of the neutrino energy, and for several values of the scattering angle θ. Starting with the solid line for $\theta = 0$, the angles from down to up correspond to $\theta = 10^o, 20^o, 30^o, 40^o$ and 50°.

with $\epsilon_{0123} = +1$ and the metric $g^{\mu\nu} = (+, -, -, -)$.

We assume that the final lepton polarization is measured in the direction defined by the vector s^μ verifying $s^2 = -1$. The polarized differential cross section (1) can be written as

$$\Sigma = \frac{1}{2}\Sigma_0 \left(1 + s_\mu P^\mu\right) \tag{4}$$

where Σ_0, given in Eq. (1), is the cross section corresponding to unpolarized leptons and P^μ is the polarization vector. The relevant components of the polarization vector in the laboratory system are defined in Fig. 1 and denoted P_l (longitudinal, in the direction of $\vec{k'}$), and P_t (transverse to $\vec{k'}$ and contained in the scattering plane). Working within the standard model, as we do in the present work, it can be shown that the polarization component perpendicular to the scattering plane (Fig. 1) is zero. [11, 36]. The expressions for the two polarization components, P_l and P_t, in terms of the hadronic structure functions

W_i are as follows

$$P_l = \mp\left\{\left(2W_1 - \frac{m_l^2}{M_i^2}W_4\right)(|\vec{k'}| - E_l'\cos\theta) + W_2(|\vec{k'}| + E_l'\cos\theta) - W_5\frac{m_l^2}{M_i}\cos\theta\right. \quad (5)$$

$$\left.\mp\frac{W_3}{M_i}((E_\nu + E_l')|\vec{k'}| - (E_\nu E_l' + |\vec{k'}|^2)\cos\theta)\right\}/F$$

$$P_t = \mp m_l\sin\theta\left(2W_1 - W_2 - \frac{m_l^2}{M_i^2}W_4 + W_5\frac{E_l'}{M_i} \mp W_3\frac{E_\nu}{M_i}\right)/F \qquad (6)$$

Note that the transverse polarization P_t is proportional to the lepton mass. The larger values of this polarization component are then expected for tau leptons, while it will be negligible for electrons at the intermediate energies of interest for neutrino reactions.
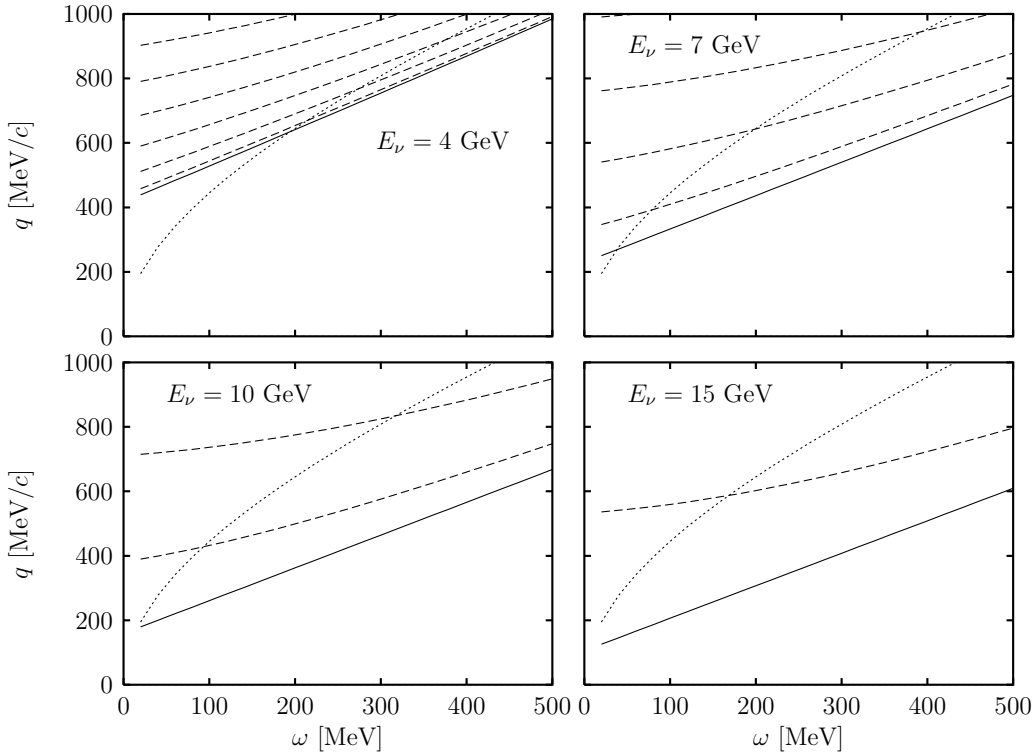

FIG. 3: Allowed kinematics for (ν_τ, τ) reaction in the (ω, q) plane. The dotted line is the center of the quasielastic peak $\omega = (q^2 - \omega^2)/2m_N$. The other lines show the value of q as a function of ω for several fixed values of the scattering angle θ. Starting with the solid line for $\theta = 0$, the angles from down to up correspond to $\theta = 2^o, 4^o, 6^o, 8^o, 10^o$ and 12°.

Let us begin with a discussion on the kinematics of the reaction in order to identify the cases of interest. For a fixed value of the neutrino energy, E_ν, and from the definition of the four-momentum transfer, $Q^\mu = K^\mu - K'^\mu = (\omega, \vec{q})$, one easily obtains the modulus of the three-momentum transfer $q \equiv |\vec{q}|$,

$$q^2 = \omega^2 - m_l^2 + 2E_\nu(E_\nu - \omega) - 2E_\nu\sqrt{(E_\nu - \omega)^2 - m_l^2}\cos\theta. \qquad (7)$$

For a fixed value of the scattering angle, the above equation gives q as a function of ω, while the case $\theta = 0$ leads to a parametrized curve corresponding to the the boundary of the

allowed kinematical region in the (ω, q) plane. The identification of this region will help in the present work because we deal with a model describing the reaction around the quasielastic (QE) peak defined by $\omega = (q^2 - \omega^2)/2m_N$, with m_N the nucleon mass. Therefore we must choose kinematics for which the QE peak lies inside the allowed region. Some examples are shown in Figs. 2 and 3 for muon and tau leptons, respectively.

In Fig. 2 the muon case is displayed for four values of the neutrino energy ranging from $E_\nu = 500$ to 1500 MeV. In each panel we show the possible kinematics in the (ω, q)-plane for several values of the scattering angle, $\theta = 10^\circ, 20^\circ, 30^\circ, 40^\circ$ and 50°. The lower solid lines correspond to the limit value $\theta = 0$, setting the lower boundary of the allowed kinematical region. The maximum value of the energy transfer $\omega_{\max} = E_\nu - m_l$ sets the right end of the boundary. In the same plots we also show the position of the maximum of the QE peak $\omega = (q^2 - \omega^2)/2m_N$ with dotted lines. Note that in all cases the QE peak region is inside the allowed region for (ν_μ, μ) reactions. In the plots we only show the low to intermediate energy transfer part $\omega < 500$ MeV since we are interested in the non relativistic regime where our nuclear model is safely applicable. This also means that the momentum transfer q must be below 600 or 700 MeV/c, since relativistic corrections at these values start to be important. Although our nuclear model is based on a fully relativistic description of the Fermi gas, the RPA and FSI corrections are non relativistic. Therefore for this work we are forced to kinematics with low to intermediate energy and momentum transfer. The plots in Figs 2 and 3 are very useful to this end since they give us a clear picture of the kinematical changes when the scattering angle is increased.

The case of τ leptons is considered in Fig. 3 for neutrino energies going from $E_\nu = 4$ to 15 GeV. This time the scattering angles shown are $\theta = 0, 2^\circ, 4^\circ, 6^\circ, 8^\circ, 10^\circ$ and 12°. In contrast to the muon case, for tau leptons the QE region is forbidden for some kinematics. In particular for low neutrino energy and low scattering angles. For instance, for $E_\nu=4$ GeV the maximum of QE peak is below the $\theta = 0$ curve for ω smaller than 200 MeV. In order to cover this region, one should go to momentum transfers well above 800 MeV/c, where relativity would play a role. Therefore we must go to larger neutrino energies, above ~ 7 GeV, in order to cover the QE region for small values of q and ω. Moreover, for large values of E_ν the momentum transfer strongly increases with the scattering angle, and then we force it to fall in the few degrees region to guarantee non relativistic kinematics.

III. RESULTS AND CONCLUDING REMARKS.

Our results showing the effects of the different corrections implemented into a nuclear model are summarized in Figs. 4–8. With dotted lines we show the results of our model without RPA and without FSI corrections. Hence these results account basically for the impulse approximation with neutrino-nucleon interaction of $V - A$ type. We use the Galster parameterization for the nucleon vector form factors and a dipole dependence for the axial form factor, while the pseudo-scalar form factor is related to the later by the partially conserved axial current (PCAC) hypothesis. These results include also the following effects:

1. Pauli blocking, through a LFG description of the nucleus. This implies an additional dependence on the experimental nuclear density.

2. Correct energy balance of the reaction using experimental $Q-$values. In the figures we show q as a function of ω minus the Q value.
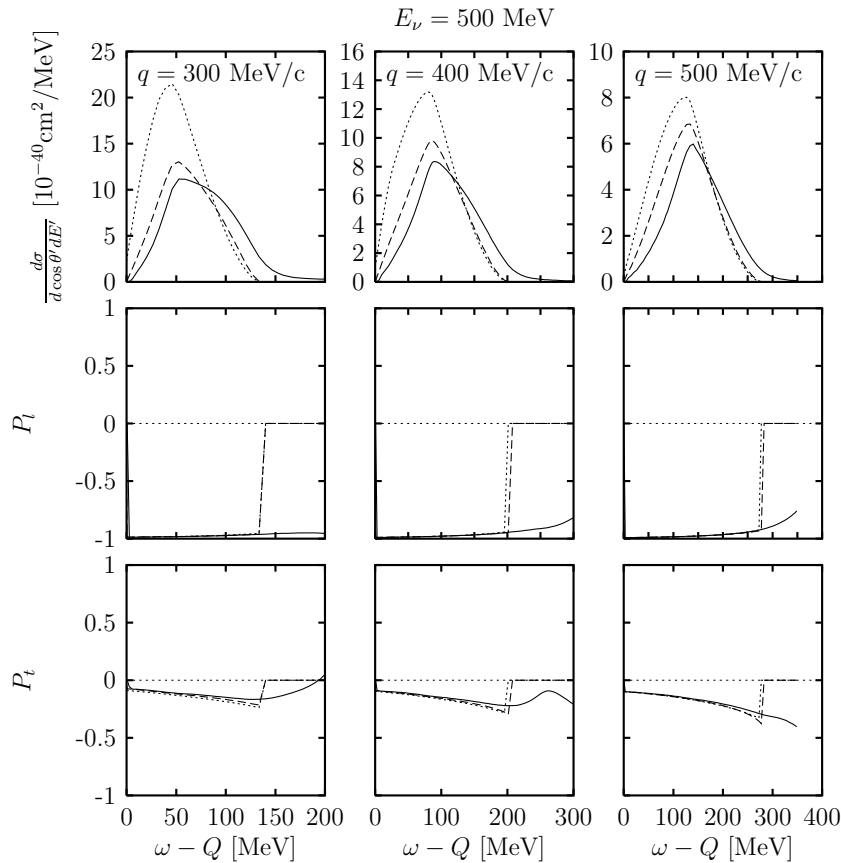
FIG. 4: Differential cross section and polarization components for the $^{40}\mathrm{Ar}(\nu_\mu,\mu)$ reaction as a function of the energy transfer minus the experimental Q-value, and for three values of the momentum transfer $q = 300, 400$, and 500 MeV/c. The incident neutrino energy is fixed to 500 MeV.

3. Coulomb distortion of the charged leptons.

More details on the parameters of CC current and on the model are given in our previous works [26, 27].

In the same plots we show with dashed lines the results including RPA corrections, that take into account modification of the nuclear medium through interactions between particle-hole and $\Delta-$hole excitations. We use an effective nucleon–nucleon interaction, with pion and rho exchange in the vector-isovector channel, and corrections due to short-range correlations. We refer the reader to Ref. [26] for details about the RPA series and for explicit expressions of the nuclear structure functions W_i entering in the CC neutrino cross section.

Finally we show with solid lines the results with the full model, including also the FSI. We account for relevant reaction mechanisms where two nucleons participate, by dressing the nucleon propagators in the nuclear medium. In particular these effects change the dispersion relation of the nucleon, which in some works is taken into account by the over-simplified method of introducing an effective mass for the nucleon [33].

We start the discussion with Fig. 4 where we show typical results for the (ν_μ, μ) reaction. In the figure we show the relevant observables, namely the differential cross section and the two polarization components, P_l and P_t in the laboratory system. The neutrino energy is
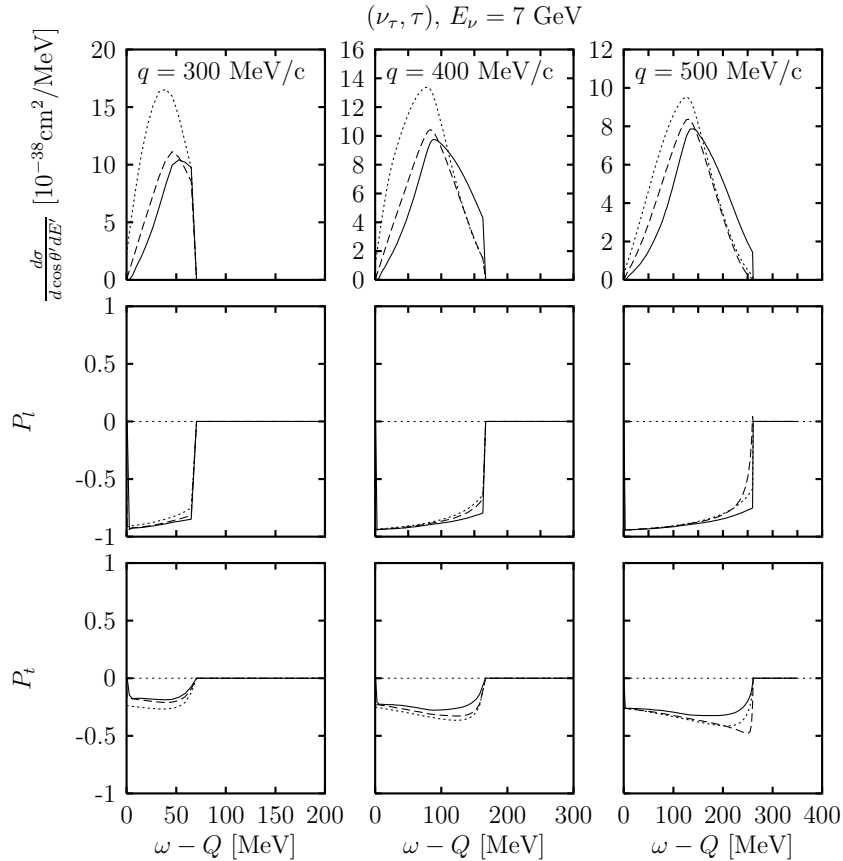
FIG. 5: The same as Fig. 4 for tau neutrinos of 7 GeV.

500 MeV, and three values of the momentum transfer $q = 300$, 400 and 500 MeV/c are considered. These values of the momentum transfer correspond to lepton scattering angles of 30° and above. The cross section shows the typical behavior of the QE peak and we can see how the different nuclear effects modify this observable. First the RPA produces a big reduction and small shift of the peak (compare the dotted to the dashed lines). The quenching of the cross section is large for low momentum transfer (almost a 50% reduction at the peak for $q = 300$ MeV/c) and diminishes with q (below 15% for $q = 500$ MeV/c). On the other hand the FSI produces a further reduction of the RPA results and an important enhancement for high energy transfer. This a consequence of the modification of the nucleon dispersion relation in the medium through the dressed nucleon propagator inside the nucleus.

Concerning the polarization observables, we see that the longitudinal component P_l is very close to -1 for the three kinematics, while there is a small but appreciable transverse component (around -0.2), quite independent of q. The inclusion of the RPA does not change these results. The reason is that the polarization components are obtained as a ratio between linear combinations of nuclear structure functions and the RPA changes similarly numerator and denominator. The same can be said for the FSI effects, except for the high-ω region. The LFG is unable to contribute to the high energy tail of the cross section, while the model with FSI is able to describe this region where, however, the QE cross section is rather small.
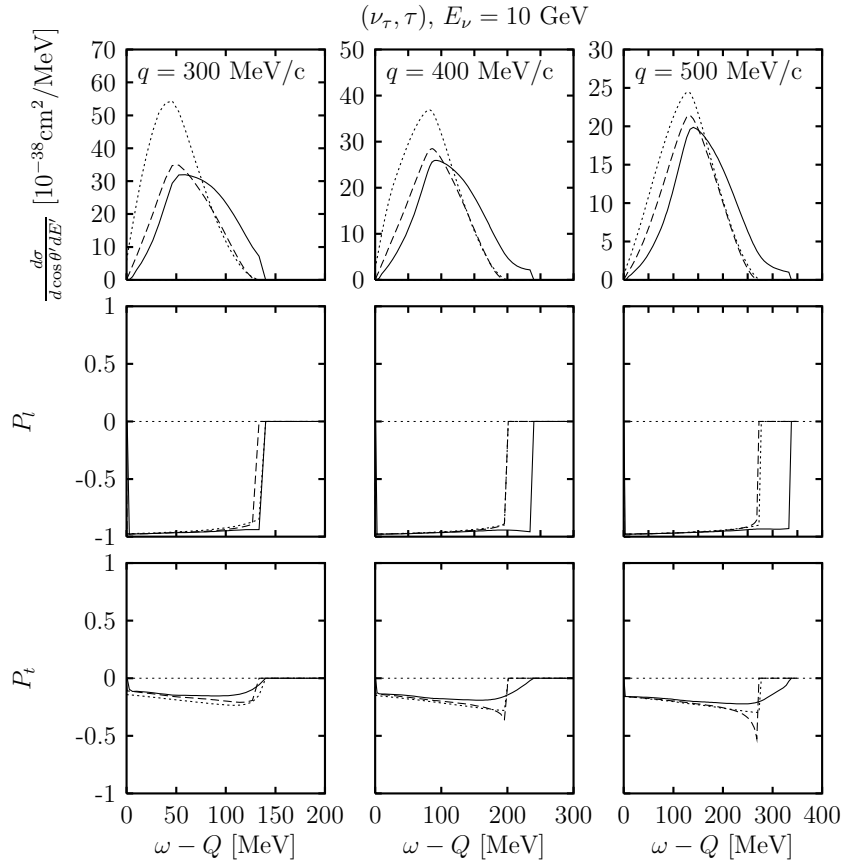
FIG. 6: The same as Fig. 5 for tau neutrinos of 10 GeV.

We have generated results for higher values of the muon-neutrino energy corresponding to the kinematics of Fig. 2. However in all the remaining cases the transverse polarization component computed is negligible and the muon can be considered polarized with negative helicity.

An example of the results found for tau leptons is displayed in Fig. 5, where we show the (ν_τ, τ) cross section and polarization observables for the same values of q as in Fig. 4, but this time for $E_\nu = 7$ GeV. By inspection of Fig. 3 we see that for the three values of q considered the maximum of the QE lies inside the allowed kinematical region. The case $q = 300$ MeV/c is closer to the boundary, since the cross section suddenly ends soon above the maximum, while for higher values of the momentum transfer the allowed region extends to higher energy transfer. The effects seen here over the cross section due to RPA and FSI are similar to the muon case studied above, with the exception of the missing high energy tail that lies now in the forbidden region.

Concerning the polarization components, the longitudinal one is still negative but now is well above -1. On the other hand, an appreciable P_t component appears, taking values ranging from ~ -0.2 to ~ -0.25. Thus the magnitude of P_t increases with q, and, as in the muon case, the RPA and FSI effects are rather small on the polarization observables.

A more clear scene with similar results can be seen in Fig. 6 for $E_\nu = 10$ GeV, corresponding to the kinematics of the third panel in Fig. 3. In this case the QE peak is well inside the allowed region for the three values of q. The polarization component P_l is now
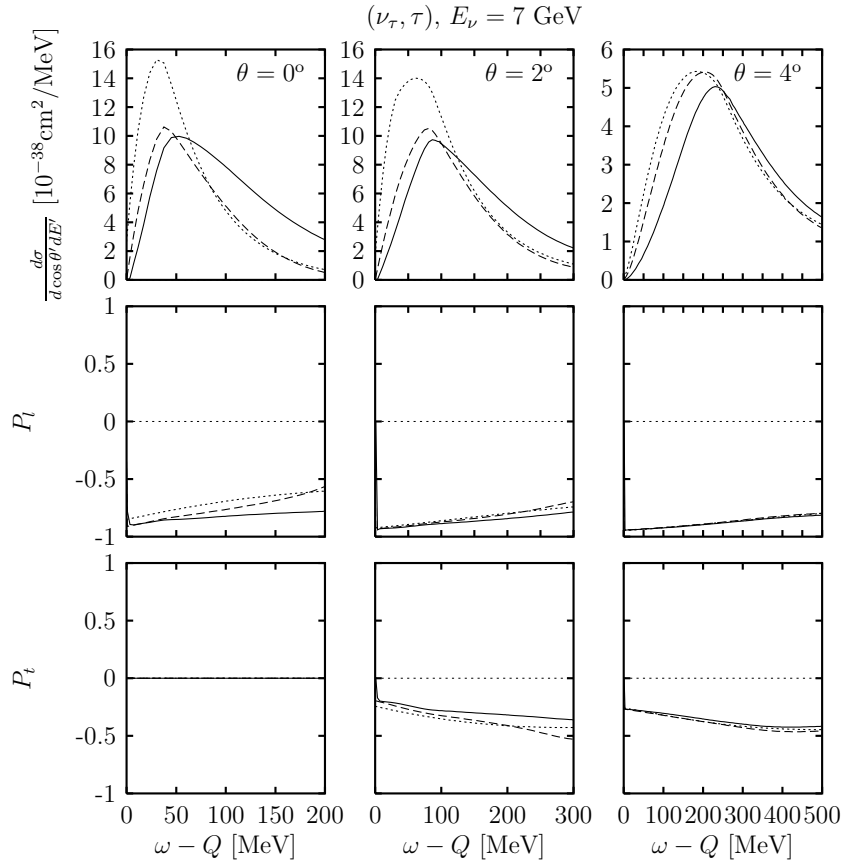
FIG. 7: The same as Fig. 5 fixing the scattering angle θ instead of the momentum transfer q. Three values of $\theta = 0^{\rm o}, 2^{\rm o}$ and $4^{\rm o}$ are shown.

closer to -1, while the magnitude of P_t is smaller than in the former case. Results for $E_\nu = 15$ GeV (not shown) indicate that P_l almost reaches the limit value ~ -1, while P_l becomes very small for high neutrino energy, as expected.

Another kind of plot of interest for ongoing neutrino experiments is shown in Fig. 7 for τ neutrinos with energy of 7 GeV. This time we fix the scattering angle instead of the momentum transfer. Therefore by changing ω we are always inside the allowed kinematical region, running along some of the curves shown in the second panel of Fig. 3, never crossing the boundary, and the cross section is defined for every value of ω shown in the plots. Results are shown for small angles, $\theta = 0, 2^{\rm o}$, and $4^{\rm o}$, in order to reach not too high values of the momentum transfer. For these angles the maximum of the QE peak is crossed at $q \sim 300, 400$, and 600, respectively. Except for $\theta = 4^{\rm o}$ at the high ω tail where the q-values are perhaps too high, and a word of caution is needed since some important relativistic corrections are expected, we can safely trust the results for lower ω-values where q is moderately low. Again we can see the important reduction of the cross section due to RPA correlations for low ω. The magnitude of this reduction decreases with the scattering angle. The FSI produces a reduction for low ω and an increase for high values of the energy transfer. The polarization component P_l is more or less independent on the angle and takes values between -0.9 and -0.8. The transverse polarization P_t is zero for $\theta = 0$ by definition, Eq. (6), while it is not negligible at all for the remaining angles, taking values between ~ -0.2 and -0.5. Concern-
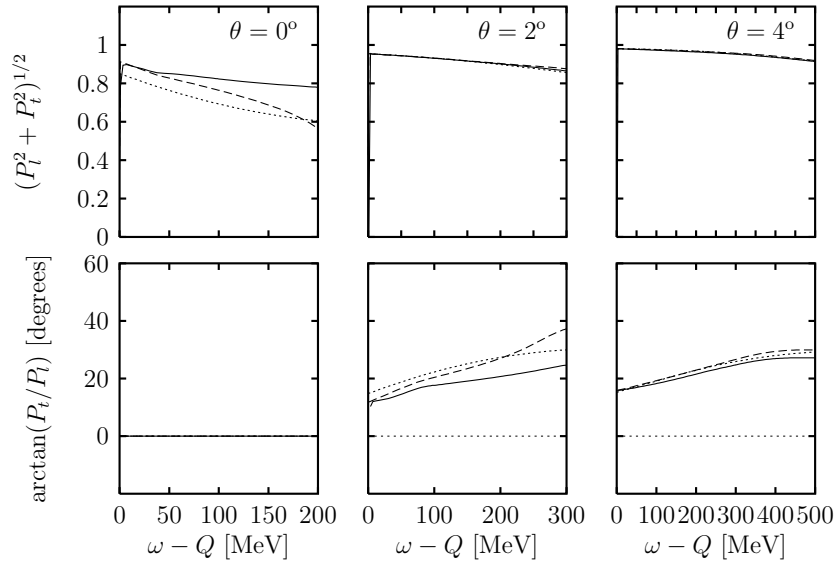
FIG. 8: Modulus and angle of the polarization vector with respect to the $-l$ direction for tau neutrinos of energy 7 GeV, and for three scattering angles, corresponding to the kinematics of fig. 7.

ing the RPA and FSI corrections on these polarization observables, the effect is found to be negligible for low energy. However at the high energy tail and for $\theta = 0$ the net RPA+FSI effect makes P_l to change from ~ -0.6 to ~ -0.8. A less important, but still appreciable change is found in P_t for $\theta = 2°$. For higher values of the scattering angle the effect is again negligible.

To end the discussion, in Fig. 8 we show another representation of polarization observables, namely, the total polarization, defined as the modulus of the polarization vector

$$|\vec{P}| = \sqrt{P_l^2 + P_t^2},$$

and the angle with respect to minus the longitudinal direction $(-\vec{k'})$,

$$\Theta \equiv \arctan(P_t/P_l).$$

The total polarization $|\vec{P}|$ takes values between 0.8 and 0.9 for $\theta = 0$ and increases with the scattering angle. For $\theta = 0$ the angle Θ is also zero, meaning that the polarization vector points to the $-\vec{k'}$ direction, without transverse components. In this case the total polarization has the meaning of fraction of particles with negative helicity. A value different from unity means that the interaction with the nuclear target produces a small fraction of tau leptons with *positive helicity*. A value close to one means that a large percentage of the leptons exit with the spin pointing to the same direction. The most probable direction of the lepton spin is determined by the angle Θ. For $\theta = 2°$ this angle is between ~ 15 and $25°$, and slightly increase for $\theta = 4°$. The results of Fig. 8 are showing a non negligible increase of the total polarization due to RPA+FSI effects, for $\theta = 0$. These effects are negligible over this observable for $\theta = 2$ and $4°$. On the other hand, for $\theta = 2°$ we find an appreciable reduction of the polarization angle Θ due to RPA+FSI, that again is negligible for higher scattering angles.

Summarizing this work, we have computed the cross section and polarization observables for neutrino induced CC reactions in nuclei at the QE peak. We have focused this work on the case of τ leptons of interest for neutrino oscillation experiments. The RPA plus FSI nuclear effects have been evaluated for intermediate energy and momentum transfer. These corrections are essential in the cross section, especially for low energy, but are partially reduced, due to cancellations, on the polarization observables. However, we have identified some particular kinematics, at very low scattering angles, where these nuclear corrections are of some importance to determine the correct magnitude and angle of the polarization vector.

Acknowledgments

[1] Super-Kamiokande Collaboration (Y. Fukuda et al.,) Phys. Rev. Lett. **81** (1998) 1562;

[2] Y. Fukuda *et al.*, Phys. Lett. B **433**, 9 (1998).

[3] A. Strumia and F. Vissani, hep-ph/0606054.

[4] The ICARUS Collaboration: F. Arneodo et al., hep-ex/0103008.

[5] M. Dracos (on behalf of the OPERA Collaboration), Phys. Atom. Nucl., 67 (2004) 1092.

[6] see `http://proj-cngs.web.cern.ch/`

[7] M. Komatsu, Nucl. Phys. B (Proc. Suppl.) 112 (2002) 15.

[8] P. Migliozzi, Int. Jou. Mod. Phys. A, 18 (2003) 3877

[9] G. Rosa, Nucl. Phys. B (proc. Suppl.) 145 (2005) 98

[10] K. Hagiwara, K. Mawatari, H. Yokoya, Nucl. Phys. B 668 (2003) 364.

[11] K. S. Kuzmin, V. V. Lyubushkin and V. A. Naumov, Mod. Phys. Lett. A **19** (2004) 2919.

[12] K. Hagiwara, K. Mawatari, H. Yokoya, Nucl. Phys. B (Proc Suppl.) 139 (2005) 140.

[13] K. Kurek, Nucl. Phys. B (Proc Suppl.) 139 (2005) 146.

[14] K.M. Graczyk, Nucl. Phys. B (Proc Suppl.) 139 (2005) 150.

[15] K.S. Kuzmin, V.V. Lyubushkin, V.A. Naumov, Nucl. Phys. B (Proc Suppl.) 139 (2005) 154.

[16] A.C. Hayes and I.S. Towner, Phys. Rev. C **61**, 044603 (2000).

[17] L.B. Auerbach et al., Phys. Rev. C **66**, 015501 (2002).

[18] C. Maieron, M. C. Martinez, J. A. Caballero and J. M. Udias, Phys. Rev. C **68**, 048501 (2003)

[19] A. Meucci, C. Giusti and F.D. Pacati, Nucl.Phys. **A739**, 277 (2004).

[20] J.E. Amaro, M.B. Barbaro, J.A. Caballero, T.W. Donnelly A. Molinari, and I. Sick, Phys. Rev. C **71**, 015501 (2005)

[21] J.E. Amaro, M.B. Barbaro, J.A. Caballero, T.W. Donnelly, C. Maieron, Phys. Rev. C **71**, 065501 (2005)

[22] J.A. Caballero, J.E. Amaro, M.B. Barbaro, T.W. Donnelly, C. Maieron, J.M. Udias, Phys. Rev. Lett. **95**, 252502 (2005)

[23] J.E. Amaro, M.B. Barbaro, J.A. Caballero, T.W. Donnelly, Phys. Rev. C **73**, 035503 (2006).

[24] M.C. Martinez, P. Lava, N. Jachowicz, J. Ryckebusch, K. Vantournhout, J.M. Udias, Phys. Rev. C73 (2006) 024607

[25] T. Leitner, L. Alvarez-Ruso, U. Mosel, nucl-th/0601103, to appear in Phys. Rev. C

[26] J. Nieves, J. E. Amaro, and M. Valverde, Phys. Rev. C **70**, 055503 (2004) [Erratum-ibid. C **72**, 019902 (2005)].

[27] M. Valverde, J. E. Amaro, and J. Nieves, Phys. Lett. B xxxx(2006) xxxx.

[28] A. Gil, J. Nieves and E. Oset, Nucl. Phys. **A627** (1997) 543; *ibidem*, Nucl. Phys. **A627** (1997) 599.

[29] R.C. Carrasco and E. Oset, Nucl. Phys. **A536** (1992) 445.

[30] E. Oset, H. Toki and W. Weise, Phys. Rep. **83** (1982) 281.

[31] L.L. Salcedo, E. Oset, M.J. Vicente-Vacas and C. García Recio, Nucl. Phys. **A484** (1988) 557; J. Nieves, E. Oset, C. García-Recio, Nucl. Phys. **A554** (1993) 509; *ibidem* Nucl. Phys. **A554** (1993) 554; J. Nieves and E. Oset, Phys. Rev. **C47** (1993) 1478; E. Oset, P. Fernández de Córdoba, J. Nieves, A. Ramos and L.L. Salcedo, Prog. Theor. Phys. Suppl. **117** (1994) 461; C. Albertus, J.E. Amaro and J. Nieves, Phys. Rev. Lett. **89** (2002) 032501; *ibidem* Phys. Rev. **C67** (2003) 034604.

[32] J. Nieves, M. Valverde, and M.J. Vicente-Vacas, Phys. Rev. C **73**, 025504 (2006).

[33] K.M. Graczyk, Nucl. Phys. A 748 (2005) 313.

[34] K.M. Graczyk, J.T. Sobczyk, Eur.Phys.J. C 31 (2003) 177.

[35] K.M. Graczyk, nucl-th/0401053.

[36] C. H. Llewellyn Smith, Phys. Rept. **3** (1972) 261.